



Shifting climate zones and expanding tropical and arid climate regions across Kenya (1980–2020)

Ted J. Lawrence¹ · Justin M. Vilbig¹ · Geoffrey Kangogo² · Eric M. Fèvre^{3,4} · Sharon L. Deem⁵ · Ilona Gluecks⁴ · Vasit Sagan^{1,6} · Enbal Shacham^{1,2}

Received: 25 June 2022 / Accepted: 4 March 2023 / Published online: 5 April 2023
© The Author(s) 2023

Abstract

Human-induced climate change significantly alters the spatiotemporal characteristics of climate zones, which drives agricultural land use and ecosystem change. However, the detectability of shifting climate zones and the rate and time of the changes has yet to be adequately addressed at the regional-to-local scale. We mapped and analyzed changes to temperature and precipitation across Kenya during the past four decades, and linked those changes to shifts in the geographic distribution and arrangement of climate zones at regional scales. We observed an approximate 1 °C increase in average annual temperature over the 40-year period. A total of 76,346 km² shifted from cooler to hotter zones, while 1298 km² shifted from hotter to cooler zones. Tropical climate regions expanded from 91 to 93%, with over 13,000 km² shifting from alpine and temperate to tropical regions. Average annual precipitation demonstrated little or no trend, but substantial spatial changes were observed. A total of 136,129 km² shifted from wetter to drier zones, while 23,317 km² shifted from drier to wetter zones. Arid climate regions expanded from 72 to 81%, a roughly 50,000 km² shift from humid and semi-humid-to-semi-arid to arid regions. Overall, there was a 207,557 km² shift in temperature and precipitation zones. As the climate zones predominately shift toward hotter and drier conditions, climatic diversity will decline, and in turn, ecosystem diversity and the ecosystem goods and services to society will decline. The changes also have broader global implications in terms of their contribution to global drylands as well as influencing earth system cycles. Overall, such information can better inform the Kenyan National Climate Change Response Strategy and be used to reach the UN Sustainable Development Goals.

Keywords Climate zones · Climate change · Spatiotemporal patterns · Socio-environmental change

Communicated by George Zittis

✉ Ted J. Lawrence
TJL222@cornell.edu

Justin M. Vilbig
justin.vilbig@slu.edu

Geoffrey Kangogo
geoffrey.kangogo@slu.edu

Eric M. Fèvre
eric.fevre@liverpool.ac.uk

Sharon L. Deem
deem@stlzoo.org

Ilona Gluecks
i.gluecks@cgiar.org

Vasit Sagan
vasit.sagan@slu.edu

Enbal Shacham
enbal.shacham@slu.edu

- ¹ Taylor Geospatial Institute, Saint Louis University, St. Louis, MO, USA
- ² College of Public Health and Social Justice, Saint Louis University, St. Louis, MO, USA
- ³ University of Liverpool, Liverpool, UK
- ⁴ International Livestock Research Institute, Nairobi, Kenya
- ⁵ Institute for Conservation Medicine, Saint Louis Zoo, St. Louis, MO, USA
- ⁶ Department of Earth & Atmospheric Sciences, Saint Louis University, St. Louis, MO, USA

Introduction

The Intergovernmental Panel on Climate Change (IPCC) Sixth Assessment Report, 2021 concluded that human activities are unequivocally causing present-era climate change (Mailloux et al. 2021), which already has led to substantial shifts in climatic conditions across large regions of the planet that are expected to continue (Cui et al. 2021). Climate zones characterize regionally similar features of the complex climate system and fundamentally shape environmental patterns and human activities at local, regional, and global scales (Li et al. 2021). However, human-induced climate change significantly alters the spatiotemporal characteristics of climate zones (Mahlstein et al. 2013). Furthermore, changes to climate zones alter the biological and physical properties of ecosystems (e.g., phenology, soil texture and structure), impact biophysical processes (e.g., carbon and nutrient dynamics), lead to additional changes and uncertainties in ecosystems, and in turn influence the capacity of ecosystems to provide goods and services to society (Hao et al. 2017). Yet, the detectability of shifting climate zones and the rate and time of the changes remains a challenge (Cui et al. 2021).

The expansion of global drylands under climate change is particularly concerning. Global drylands cover about 41% of the Earth's land surface (FAO 2019), have expanded over the latter half of the twentieth century (Feng and Fu 2013), and are projected to expand 10–15% during the twenty-first century (Li et al. 2021; Yao et al. 2020). Africa has one of the most extensive dryland systems, which comprises roughly 15% of the global land area (Právělie 2016). West Africa is projected to evolve towards increasingly hot and dry zones with the recession of cool and wet zones (Sylla et al. 2016). Drylands in East Africa face potential expansion with drought areas likely to increase 16–54% during the twenty-first century, which would gradually exacerbate land degradation and desertification (Haile et al. 2020). The expansion of drylands is predominantly the result of changes to climate zones, from cool and wet zones to hot and dry zones (Burrell et al. 2020).

Few studies have empirically examined the shift in climate zones, from cool and wet to hot and dry zones due to human-induced climate change. Most studies have concentrated on individual impacts, such as heat extremes (Dosio et al. 2018), drought (Naumann et al. 2018), flooding, and water resources (Gosling and Arnell 2016). Furthermore, most studies solely focus on climatological metrics that do not necessarily represent biomes or the different types of ecosystems (Mahlstein et al. 2013). Yet, climate zones play an essential role in impact assessments of climate change on social and ecological systems (Akter et al. 2020; Guo et al. 2021; Hunter et al. 2021; Wang et al. 2019; Yang

et al. 2021). Thus, climate zones can be used to assess climate change impacts on living environments (Li et al. 2021), help policymakers develop strategies for the most vulnerable areas, and to address UN Sustainable Development Goals (Fonseca et al. 2020; Sylla et al. 2016).

It is important to develop an understanding of climate zones that is practical, effective, and integrates the most up-to-date knowledge to produce high resolution and spatially explicit projections of current climate zones (Le Page et al. 2017). Climate zone classification and change analysis are necessary steps towards understanding the complex spatiotemporal interactions between different climatic variables (Guan et al. 2021). Furthermore, understanding how climate change alters the spatiotemporal distribution of climate zones is an important question of great practical and scientific interest that has yet to be adequately addressed (Li et al. 2021).

Our objective for this study is to understand how human-induced climate change has impacted climate zones across Kenya. Focusing our study on Kenya was important because rain-fed agriculture is central to the country's economy, comprising one third of its GDP and employing more than half its labor force (Nechifor et al. 2021). Furthermore, Kenya is a key food-producing country for the East African region and a key player in regional food security (Eichsteller et al. 2022). Kenya's high level of biodiversity also is under threat from a myriad of sources, including ecosystem degradation, water scarcity, and habitat fragmentation, which are exacerbated by climate change and shifting climate zones (Jenkins et al. 2021). Therefore, our research questions are as follows: (1) how have temperature and precipitation trends changed over time in Kenya; and (2) how have the geographic distribution and arrangement of climate zones in Kenya shifted over time due to the changes in temperature and precipitation?

Study area, data, and methods

Study site: Kenya

Located in East Africa, Kenya lies on latitude 5°S–5°N and longitude 34°E–42°E. Kenya covers approximately an area of 583,000 km², which comprises a land surface of roughly 98% with the remaining areas as water bodies (Kogo et al. 2021). A large fraction of Kenya's region has been categorized as arid or semi-arid with only 15% suitable and fully used for agricultural production and roughly 80% being rangelands for the roughly 50 million human population of Kenya (Koeva et al. 2020). Despite the relative aridity, Kenya's arid and semi-arid regions accommodate about 25% of Kenya's human population, 60% of the livestock population, and the largest proportion of wildlife (Ngugi and Nyariki 2005).

Proximity to the equator, the Indian Ocean, and the Inter-tropical Convergence Zone (ITCZ) influences Kenya's climate

(CDKN 2012). The rainfall patterns are governed by the seasonal variability and intensity of the ITCZ due to differences in altitude with long rains often occurring from March to May and short rains occurring from September to December (Nicholson 2018), although atmospheric dynamics in the first month (September) differ from the rest of the rainy season (Shongwe et al. 2011). The long and short rains as well as variations in average monthly temperatures generally follow the four standard seasons of December through February, March through May, June through August, and September through November (Kogo et al. 2021). Moreover, the country exhibits a wide range of climate conditions, comprising a large diversity of climate zones, with a temperature gradient from alpine, to temperate, to tropical regions, and a precipitation gradient from humid, to semi-humid-to-semi-arid, to arid regions (Gikonyo et al. 2018). In recent years, climate change has been experienced through more frequent and extreme climate events, such as droughts and floods (Kogo et al. 2021). In turn, households in Kenya are facing challenges in adapting to the ever-changing climatic conditions with limited capacity and resources to cope with dire consequences on their agricultural productivity (Bryan et al. 2013).

Agricultural activities in Kenya are organized according to agro-climatic zones (ACZs), which are the delineation of landscapes into regions with relatively homogeneous and contiguous areas based on similar climate characteristics (Kogo et al. 2021). Kenya is divided into roughly forty ACZs, which were designated circa 1980 and documented by a report of Kenya's Ministry of Agriculture (Sombroek et al. 1982). Each ACZ comprises a moisture zone reflecting mean annual rainfall and overlapped with a temperature zone reflecting mean annual temperature for a total of 7 moisture zones and 9 temperature zones (Gikonyo et al. 2018). In all, the ACZs represent a temperature gradient from alpine, to temperate, to tropical regions, and a moisture gradient from humid, to semi-humid-to-semi-arid, to arid regions.

Data collection and description

Data utilized in this study included (1) average monthly and annual temperature and precipitation time series of Kenya between 1975 to 2020 that was obtained from the Climate Change Knowledge Portal (CCKP 2022), which is a web-based platform and hub for climate-related information, data, and tools that provides global data on historical and future climate, vulnerabilities, and impacts; (2) georeferenced average monthly temperature and precipitation across Kenya with a 5-km resolution during 1976–1980, 1996–2000, and 2016–2020 from the TerraClimate dataset (Abatzoglou et al. 2018), which was accessed through Google Earth Engine (GEE: Gorelick et al. 2017) and lends itself to temporal high-resolution analysis more so than other similar datasets; and (3) a digitized version of the georeferenced boundaries

of the Kenyan ACZs that were documented in 1982, which was obtained from the IGAD Climate Prediction and Applications Centre Portal (ICPAC 2022).

Kenya's climate trends and mapping temperature and precipitation patterns

First, using the CCKP time series, we assessed the average annual and seasonal temperature and precipitation trends across Kenya to understand climate change in the country between 1975 and 2020. Furthermore, we tested the magnitude in the trends and their significance based on the Sen slope estimator (Sen 1968) and modified Mann–Kendall test (Hamed and Rao 1998) technique. Next, we created climate reference maps with three raster images representing precipitation patterns and three raster images representing temperature patterns in Kenya of approximately 1980, 2000, and 2020 based on the TerraClimate dataset using GEE. Given that we observed high inter-annual rainfall variability in Kenya based on the CCKP time series, the raster images representing precipitation patterns were created through calculating the median pixel values of monthly precipitation over the 4 years preceding and including 1980, 2000, and 2020. Observing little inter-annual variability in temperature, the raster images representing temperature patterns were created through calculating the median pixel values of monthly temperature within 1980, 2000, and 2020.

Assessing temperature and precipitation patterns within Kenya's agro-climatic zones

We mapped and analyzed temperature and precipitation within Kenya climate zones in 1980 and linked the patterns to shifts in the geographic distribution and arrangement of climate zones at regional scales over 40 years since 1980. We used the georeferenced boundaries of the Kenyan ACZs to represent climate zones in 1980 because their formation was based primarily on regionally similar patterns of precipitation and temperature. Using the 1980 climate reference maps, we assessed temperature patterns within each ACZ temperature zone and precipitation patterns within each ACZ moisture zone via ArcGIS Pro 2.9.2 (ESRI 2022). Specifically, we assessed the distribution (mean and standard deviation) of temperature and precipitation within each respective temperature and moisture zone, compared the distributions to average temperature and precipitation information provided in the original ACZ map from Sombroek et al. (1982), and developed discrete average ranges of both climate variables within each zone to represent temperature and precipitation zones (Table 1). Also, we assigned climatic designations to the zones based on information from the original ACZ map in Sombroek et al. (1982) and the Köppen–Geiger climate classification (Beck et al. 2018).

Creating and assessing classified maps of temperature and precipitation zones

We created classified maps representing temperature and precipitation zones in 1980, 2000, and 2020. First, we sampled temperature and precipitation in 1980 across the full spatial extent of each zone following our previously designated ranges shown in Table 1 with at least the recommended minimum number of 50 samples per zone (Chuvieco 2016) and each sample including multiple pixels for both climate variables. Next, the samples were used to train three classification algorithms: maximum likelihood (ML, Eq. 1); support vector machine (SVM, Eq. 2); and random forest (RF, Eq. 3) in ArcGIS Pro (Rana and Venkata Suryanarayana 2020; Additional details are provided in Appendix A).

Equation 1 Maximum likelihood

$$p(x) = \sum_{i=1}^m p(x|w_i)p(w_i) \quad (1)$$

where

$p(x|w_i)$ are the set of class conditional probabilities
 $p(w_i)$ is the probability that cells from class w_i appear anywhere in the image.

Equation 2 Support vector machine

$$\mathbf{w}^T \mathbf{x} - \mathbf{b} = 0 \quad (2)$$

where

\mathbf{w} is the normal vector of the hyperplane.
 \mathbf{x} is a set of points x .
 and
 $(x_1, y_1), \dots, (x_n, y_n)$ is a training dataset of n points, where y_i are either 1 or -1 , each indicating the class to which the point x_i belongs.

Equation 3 Random forest

$$\{h, (x, \theta k), k = 1, \dots, \} \quad (3)$$

where

\mathbf{x} is the input vector.

θ_k are the independent and identically distributed random vectors.

We then created classified maps of temperature and precipitation zones in 1980 for each classification algorithm. Following the supervised classification process and based on Olofsson et al. (2014), we conducted an assessment of each classification between the coarse-scale, multi-pixel model, and the 1980 climate reference maps at a finer, pixel-level resolution, and excluded the training sample areas to measure the level of agreement using ArcGIS Pro and Python scripting in Google Colab. While Eqs. 4 and 5 were applied in the assessment, additional details about the assessment are provided in Appendix B.

Equation 4 Producer's accuracy (PA_i)

$$A_i = \frac{X_{ii}}{X_{+i}} P \quad (4)$$

where

x_{ii} is the diagonal of each column of the error matrix.

x_{+i} represents the total of column i .

Equation 5 User's accuracy (UA_i)

$$UA_i = \frac{X_{ii}}{X_{i+}} \quad (5)$$

where

x_{ii} is the diagonal of each row of the error matrix.

x_{i+} represents the total of row i .

We designated 100 random assessment points for each zone because it is twice the recommended minimum number of training samples (50 per zone) to obtain a reliable estimation of error (Chuvieco 2016). We evaluated the assessments using error matrices, an overall assessment score, confidence intervals, and kappa statistic (Eqs. 6–8 with additional details in Appendix C). Finally, and based on the

Table 1 Temperature and precipitation ranges within each Kenyan agro-climatic zone to analyze the change in the pattern and distribution of the agro-climatic zones over 40 years

Precipitation Zone	Average Precipitation (mm)	Climatic Designation	Temperature Zone	Average Temperature (Celsius)	Climatic Designation
1	> 103	Humid	1	> 25	Tropical-fairly hot to very hot
2	80–103	Sub-humid	2	22–24	Tropical-very warm
3	65–80	Semi-humid	3	20–22	Tropical-warm
4	48–65	Semi-humid to semi-arid	4	18–20	Tropical-mild
5	36–48	Semi-arid	5	16–18	Temperate-mild
6	25–36	Sub-arid	6	14–16	Temperate - cool
7	< 25	Arid	7	12–14	Temperate - cold
			8	10–12	Temperate - very cold
			9	< 10	Alpine - extremely cold to frigid

assessment results, we applied the trained SVM algorithm to the 2000 and 2020 climate raster images to create classified maps of temperature and precipitation zones in those years. Assessments of the SVM algorithm's performance were also conducted on the 2000 and 2020 classified maps in comparison to the 2000 and 2020 climate reference maps (Appendix D).

Equation 6 Overall accuracy (OA)

$$OA = \frac{\sum_{i=1,n} x_{ii}}{\sum_{i=1,n} \sum_{j=1,n} x_{ij}} \quad (6)$$

where

x_{ii} is the diagonal of each column of the error matrix.

x_{ij} is a cell in the error matrix.

Equation 7 Kappa statistic (k)

$$k = \frac{n \sum_{i=1,n} X_{ii} - \sum_{i=1,n} X_{i+} X_{+i}}{n^2 - \sum_{i=1,n} X_{i+} X_{+i}} \quad (7)$$

where

n is the sample size.

X_{ii} indicates the observed agreement.

$X_{i+} X_{+i}$ is the product of the total row and column that estimates the expected agreement for each category i .

Equation 8 Confidence interval

$$\hat{p} \pm z \sqrt{\frac{\hat{p}(1 - \hat{p})}{n}} \quad (8)$$

where

$\hat{p} = \frac{n_1}{n}$ is the proportion of successes.

n_1 is the number of successes out of n number of trials.

z is the $1 - \frac{1}{2}\alpha$ quantile of a standard normal distribution corresponding to the error rate α .

Estimating temperature and precipitation zonal changes over time

We demonstrate the geographic changes to climate zones via the classified maps over time for temperature and precipitation zones. We conducted a post-classification comparison of the classified temperature and precipitation zone maps to detect and estimate shifts in climate zones over time. Absolute and percentage changes in each temperature and precipitation zone were calculated between 1980, 2000, and 2020. We also calculated each zone's proportion of Kenya's total land area and the change in the proportions between 1980 and 2020. Next, we disaggregated the changes into the amount of areas in km² that shifted between zones to map and analyze the change pathways. We overlaid and analyzed the change in temperature and precipitation zones to understand the overall climate zone shifts. Additionally, we calculated the changes to (1) all humid, semi-humid to

semi-arid, and arid regions; and (2) all tropical, temperate, and alpine regions.

Results

Kenya has experienced a roughly 1 °C increase in temperature since the 1970s (Fig. 1a). Similarly, there was an increasing trend in temperature across all of the four standard seasons (Fig. 1b). Average annual precipitation does not exhibit a trend between 1975 and 2016, but a slight increasing trend appears between 1975 and 2019 due to the above normal annual rainfall over the last few years (Fig. 1c). However, precipitation exhibited a decreasing trend during Kenya's primary rainy season (March through May; Fig. 1d). Alternatively, precipitation exhibited an increasing trend during most of Kenya's secondary rainy season (September through November). Furthermore, the trends in the primary and secondary rainy seasons appeared to converge in recent years. Lesser divergent trends were exhibited in the dry seasons (December through February and June through August). The regression equations for each temperature and precipitation time series and the results of testing the trends are reported in Appendix F.

The largest changes over time to the precipitation zones as proportions of the country's total area were in the semi-humid to semi-arid (zone 4), from 14% in 1980 to 8% in 2020, and in the sub-arid (zone 6), from 12% in 1980 to 18% in 2020 (Fig. 2a). Semi-arid (zone 5) expanded from 9% in 1980 to 11% in 2020, while the humid (zone 1) contracted from 5% in 1980 to 2% in 2020. Little or no change in the proportions was exhibited in the sub-humid (zone 2: constant 4%), semi-humid (zone 3: 5 to 4%), and arid (zone 7: 51 to 52%). Humid, semi-humid to semi-arid, and arid zones exhibited the largest absolute and percent changes between 1980 and 2020. Semi-humid and semi-arid zones exhibited the next largest absolute and percent changes over time. The smallest absolute and percent changes were exhibited in arid and sub-humid zones.

Figure 2b shows the location of changes between zones over the 40 years and the pathway of the absolute change for each zone that is shown in the table of Fig. 2a. Examining below the diagonal (dotted line) of the change pathway chart in Fig. 2b, the largest spatial shifts in the precipitation zones were along the borders from wetter to drier zones. A total of 115,416 km² shifted by one zone from wetter to drier, while 20,706 km² shifted by two zones from wetter to drier, and 7 km² shifted by three zones from wetter to drier. A total of 136,129 km² shifted from a wetter to a drier zone, while a total of only 23,317 km² shifted from a drier to a wetter zone. The largest spatial change was from semi-humid-to-semi-arid (zone 4) to semi-arid (zone 5) with a 33,048 km² shift. The next largest shift was 25,171 km² from semi-arid

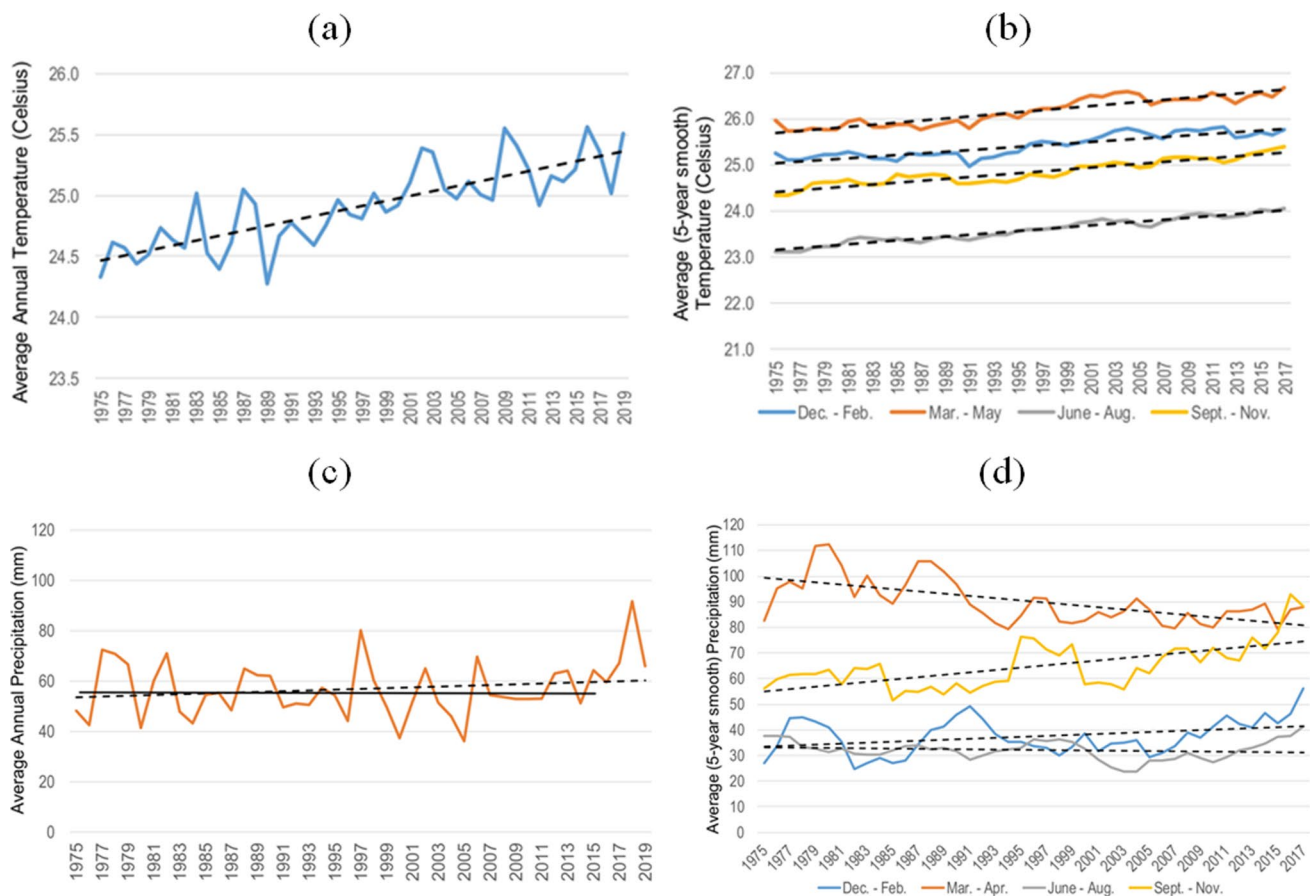


Fig. 1 Kenya's temperature and precipitation trends. Average annual temperature from 1975 to 2019 (a), 5-year rolling average of annual seasonal temperatures between 1975 and 2017 (b), average annual

precipitation from 1975 to 2019 (c), and 5-year rolling average of annual seasonal precipitation between 1975 and 2017 (d)

(zone 5) to sub-arid (zone 6). Furthermore, not only have most precipitation zones shifted from wetter to drier but also the average precipitation in arid zone (7) decreased 2.57 mm between 1980 and 2020.

Little change to temperature zones as proportions of Kenya's total area were observed. The tropical–fairly hot to very hot (temperature zone 1) expanded from 63 to 66% over the country's total land area (Fig. 3a). Tropical–warm and temperate–mild zones contracted from 8 to 7% and 6 to 4% respectively. The proportion of all other zones remained constant. The largest increase by area (17,137 km²) was exhibited in the tropical–fairly hot to very hot region (zone 1) with a small (5%) percent change. The largest decrease (7928 km²) was exhibited in the temperate–mild (zone 5) with a –25% percent change. However, the smallest percent change (0%) was exhibited in the tropical–mild (zone 4) with 146 km² increase, while the largest percent change (–54%) was in the temperate–very cold (zone 7) with a 1289 km² decrease.

Figure 3b shows the location of changes between zones over the 40 years and the pathway of the absolute change

for each zone that is shown in the table of Fig. 3a. Examining above the diagonal (dotted line) of the change pathway chart, the largest spatial shifts in the temperature zones were along the borders from cooler to warmer zones. A total of 76,287 km² shifted by one zone from cooler to warmer, while 54 km² shifted by two zones from cooler to warmer, and 5 km² shifted by three zones from cooler to warmer. A total of 76,346 km² shifted from a cooler to a warmer zone, while a total of only 1298 km² shifted from a warmer to a cooler zone. The largest spatial change was from tropical–warm (zone 3) to tropical–very warm (zone 2) with a 19,842 km² shift. The next largest shift was 17,742 km² from tropical–very warm (zone 2) to tropical–fairly hot to very hot (zone 1). Furthermore, not only have most temperature zones shifted from cooler to warmer but also the average temperature in tropical–fairly hot to very hot (zone 1) increased 0.59 °C between 1980 and 2020.

The overlap of areas that shifted between precipitation zones and that shifted between temperature zones is shown in Fig. 4. More than 200,000 km² (approximately 36%) of Kenya experienced shifts in precipitation zones only, shifts

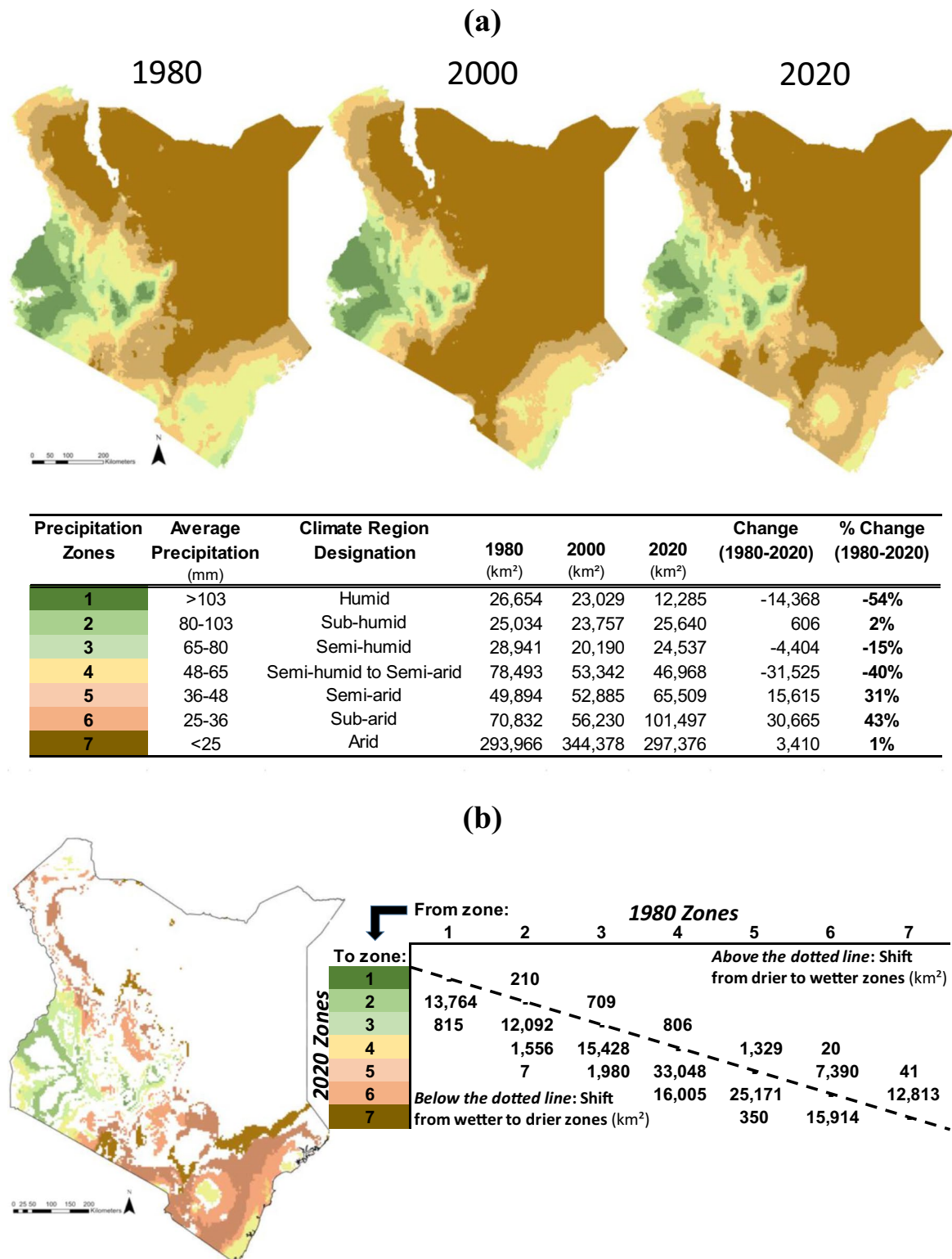


Fig. 2 Classified precipitation zones, change in areas over time, and pathway of shifting precipitation zones. Maps for each year show the spatial arrangement of the precipitation zones (a). The table of a shows the climate region designation for each zone, area (km²) of each zone in each year, the change between 1980 and 2020, and the percent change in the area of each zone over the study period. In the map of b, the colors represent zone designations in 2020 following the shift between zones.

The chart of b shows the change in km² between precipitation zones in 1980 to precipitation zones in 2020. Numbers above the dotted line represent a shift from drier to wetter zones. Numbers below the dotted line represent a shift from wetter to drier zones. The further a number is from the dotted line, the greater the shift in the number of zones. For each zone, the sum of its row minus the sum of its column equals the total change (1980–2020) for that zone shown in the table of a

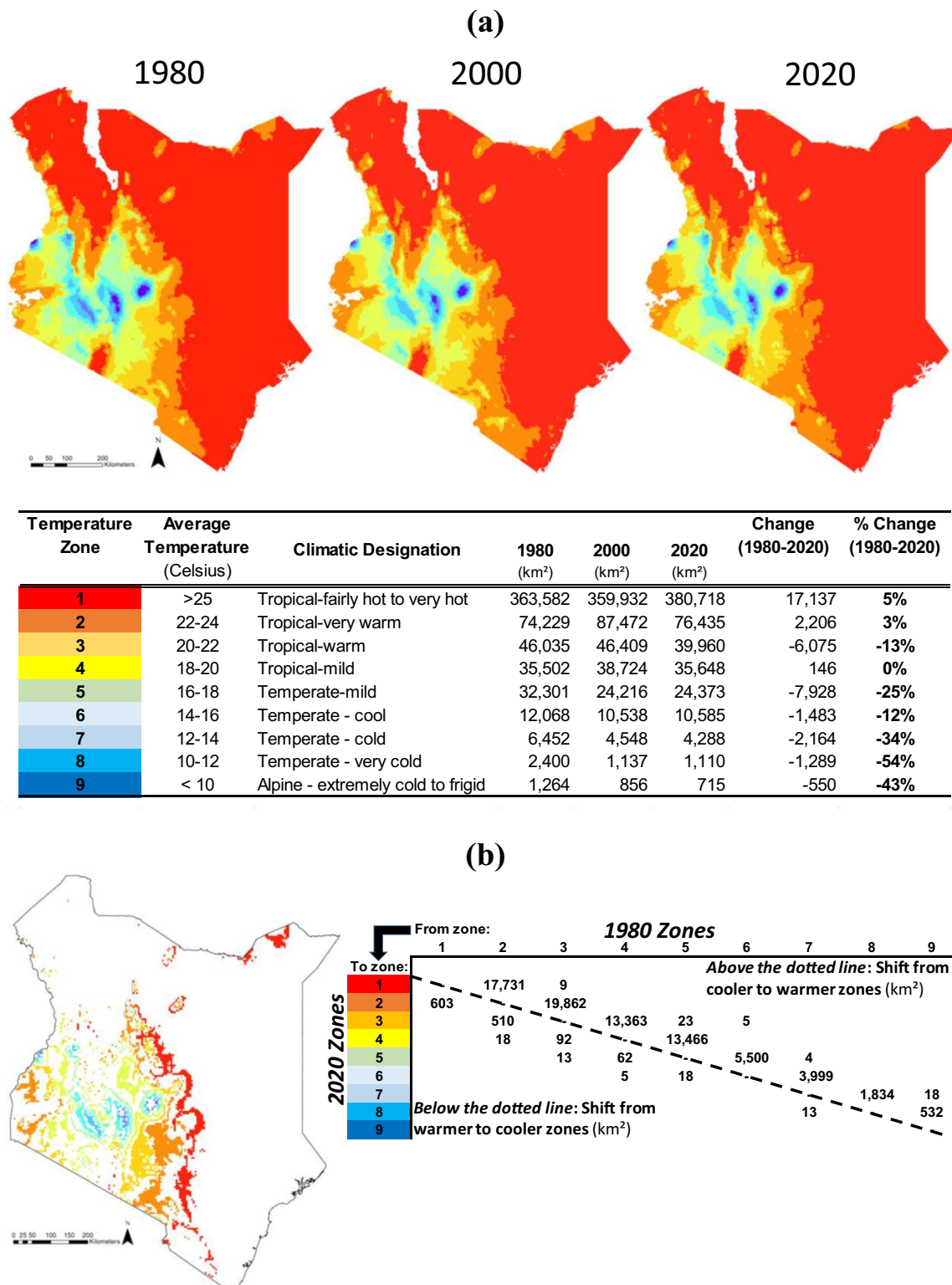


Fig. 3 Classified temperature zones, change in areas over time, and pathway of shifting temperature zones. Maps for each year show the spatial arrangement of the temperature zones **(a)**. The table in **a** shows the climate region designation for each zone, area (km²) of each zone in each year, the change between 1980 and 2020, and the percent change over the study period. In the map of **b**, the colors represent zone designations in 2020 following the shift between zones. The chart in **b** shows

the change in km² between temperature zones in 1980 to temperature zones in 2020. Numbers above the dotted line represent a shift from cooler to warmer zones. Numbers below the dotted line represent a shift from warmer to cooler zones. The further a number is from the dotted line, the greater the shift in the number of zones. For each zone, the sum of its row minus the sum of its column equals the total change (1980–2020) for that zone shown in the table of **a**

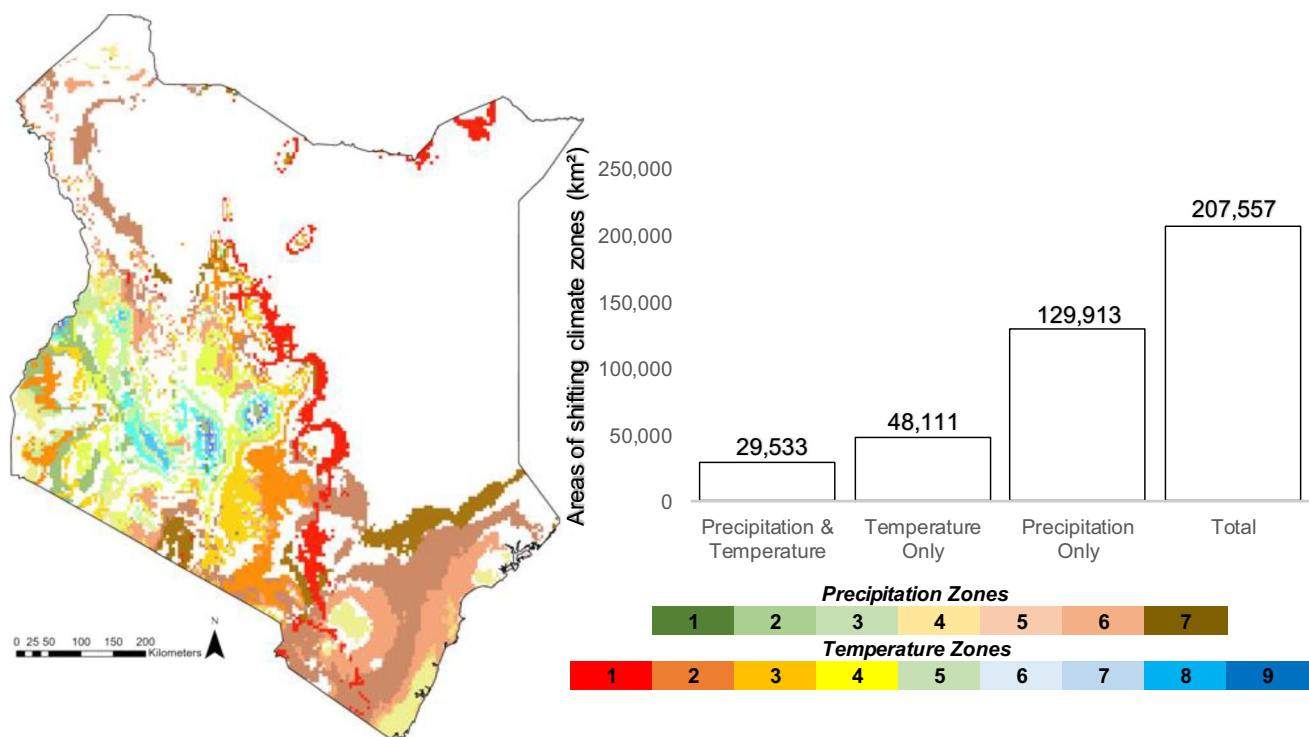


Fig. 4 Areas of shifting precipitation and temperature zones. The map shows the overlap of areas that shift between precipitation zones and that shift between temperature zones. The histogram shows the

area of shifts in: (1) precipitation and temperature zones; (2) temperature zones only; (3) precipitation zones only; and (4) total km² between temperature and precipitation zones

in temperature zones only, or shifts in both temperature and precipitation zones. The next largest area (129,913 km²) experienced shifts in precipitation zones only. A much smaller area (48,111 km²) experienced shifts solely in temperature zones. Only 29,533 km² experienced shifts in both precipitation and temperature zones.

All arid regions expanded from 414,692 km² (72% of all of Kenya's total area) in 1980 to 464,382 km² (81%) in 2020 (Fig. 5). The semi-humid to semi-arid region shrunk from 78,493 km² (14%) in 1980 to 46,968 km² (8%) in 2020. All humid regions also shrunk from 80,628 km² (14%) in 1980 to 62,462 km² (11%) in 2020. All tropical regions expanded from 519,347 km² (91% over all Kenya) in 1980 to 532,761 km² (93%) in 2020. The alpine region shrunk from 1264 km² (less than 1%) in 1980 to 715 km² in 2020. All temperate regions also shrunk from 53,220 km² (9%) in 1980 to 40,365 km² (7%) in 2020.

Discussion

Human-induced climate change across Kenya resembles global trends. In particular, the increase in average annual and seasonal temperatures mirror changes in global temperatures. However, the largest spatial shifts were in the tropical

zones, from mild to very hot temperatures. The regionality of global change suggests that certain regions are more sensitive to both natural and anthropogenic factors of climate change, which alters the energy flux in the atmosphere (Fu 2017). For example, the largest global warming during the last 100 years was observed over drylands and accounted for more than half of the continental warming (Huang et al. 2017). Thus, consensus among the scientific community is that throughout the African continent, including Kenya, the long-term increase in average annual temperature will likely be larger than the increase in average annual global temperature, with drier subtropical regions warming more than the moister tropics (Seely et al. 2008).

Precipitation zones experienced the largest overall spatial shifts across Kenya. In particular, the semi-humid to semi-arid zone in Kenya experienced the largest decrease (proportional and absolute) of all the precipitation zones, which is consistent with global patterns of transitional climate zones being the most vulnerable areas to human-induced climate change (Ayugi et al. 2016; Huang et al. 2017). Moreover, our results demonstrated that all arid regions had the largest (proportional, absolute, and percent) expansion. Such change can contribute to the expansion of drylands across Kenya, which can further lead to reduced carbon sequestration and enhanced regional warming, bolstering the warming

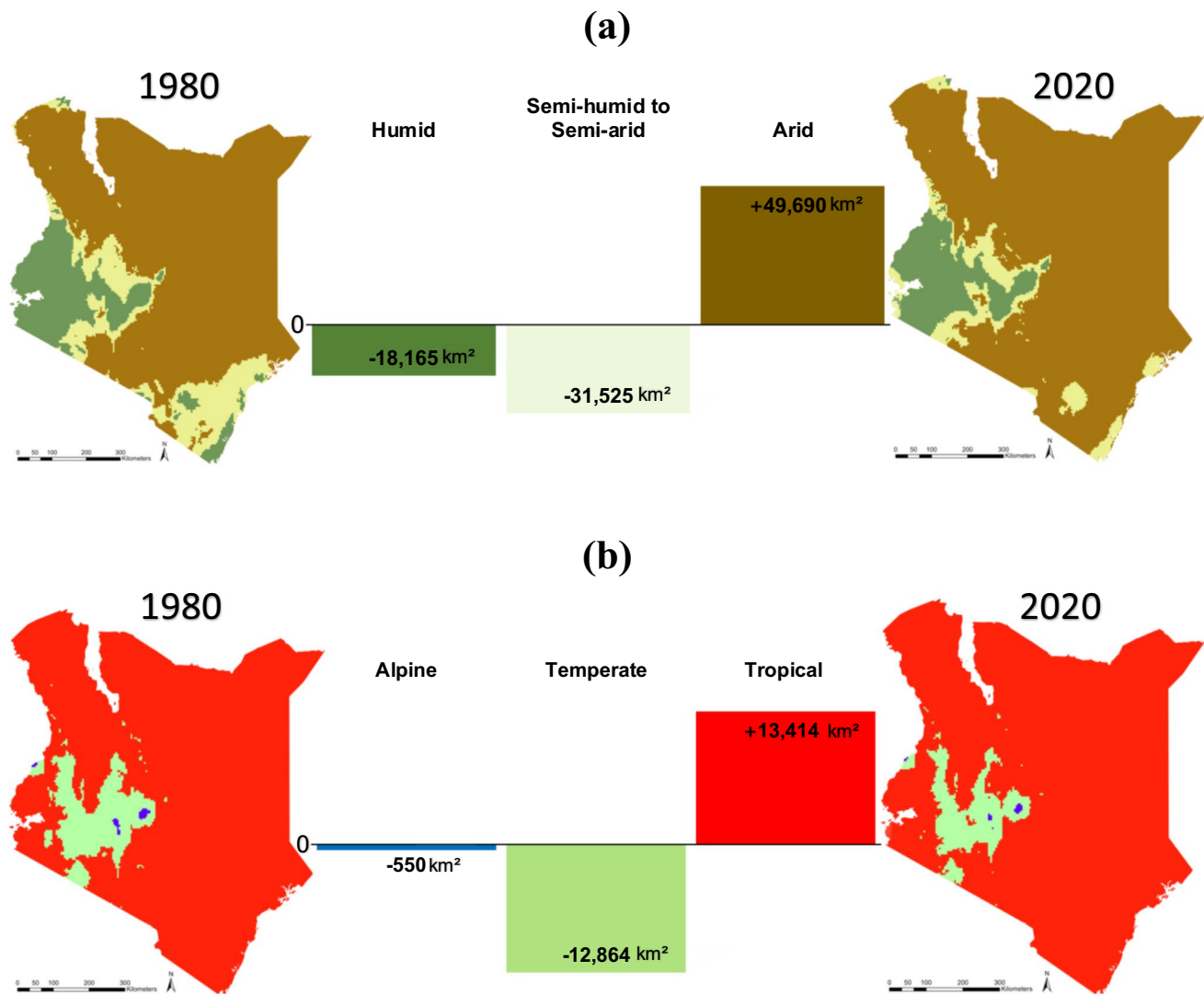


Fig. 5 Change in climate regions across Kenya from 1980 to 2020. Change in humid, semi-humid to semi-arid, and arid regions **(a)**. Humid regions include changes to humid, sub-humid, and semi-humid zones. Arid regions include changes to arid, sub-arid, and

semi-arid zones. Change in tropical, temperate, and alpine regions **(b)**. Temperate regions include changes to temperate-mild to temperate-very cold zones. Tropical regions include changes to tropical-mild to tropical-fairly hot to very hot zones

trends over the present drylands (Huang et al. 2016). Furthermore, in addition to contributing to the expansion of global drylands, Kenya's arid region can contribute to global climate change through releasing into the atmosphere the carbon stored in dryland vegetation and soils.

Increasing temperature and changes to temperature zones likely exacerbate the expansion of drylands in Kenya (Bradford et al. 2019). Specifically, drylands in arid regions are expected to dry more quickly and severely and to a greater extent than in humid regions (Yao et al. 2020). Tropical-fairly hot to very hot (temperature zone 1), which comprises a large majority of Kenya, expanded substantially more than any other temperature zone. The enhanced warming has important implications in interpreting global

warming patterns and assessing the impacts of climate change (Huang et al. 2017). Furthermore, the expansion of all tropical regions and contraction of all temperate and alpine regions in Kenya may serve as a microcosm to understanding the expansion of the global tropics, which the scientific community has struggled to characterize (Heffernan 2018).

Shifting climate zones are considered a direct measure of suitability for agriculture and ecosystems and have previously been used as an indicator for climate change threats to ecosystems (Ceglar et al. 2019). As climate zones predominantly shift toward hotter and drier conditions, climatic diversity will decline, and in turn, ecosystem diversity and the ecosystem goods and services to society will decline

(Guan et al. 2021). Particularly, shifting climate zones are expected to pose a serious threat to agricultural systems, and impact crop yields, agricultural activities, and food prices (Wang et al. 2022). Heat stress in domesticated livestock is also a major impact of changing climate zones, which can affect weight gain, milk yield, fertility, and overall animal welfare (Thornton et al. 2021; 2022). Furthermore, the emergence of vector-borne diseases have been associated with changes in temperature and humidity, which often determine suitable ecological niches for neglected tropical diseases (Ghazali et al. 2018). Overall, shifting and changing climate zones pose a major threat to terrestrial ecosystems with far-reaching social and ecological impacts (Bindhu et al. 2021; Cui et al. 2021).

Together, hotter and drier conditions, as experienced in Kenya over the 40-year study period, accelerate desertification with devastating impacts on a wide variety of land and natural resources, which further drives biological processes that can change life cycles (Spinoni et al. 2021). Similar observations of decreased rains, warming temperatures coupled with rapid population growth under a warmer climate have been observed in neighboring Uganda signaling a major regional to global challenge (Ayugi et al. 2022; Ngoma et al. 2022). Managing ecosystem change is among the greatest challenges that humanity faces in the twenty-first century (Lawrence et al. 2020), and drylands are especially prone to changes (Bestelmeyer et al. 2015). The United Nations' Sustainable Development Goals (UN-SDG) set the specific Goal 15 to combat desertification and limit its impacts (Spinoni et al. 2021). Thus, the need for insights about geographic patterns of climate vulnerability in arid regions is especially important, where degradation has been witnessed on global scales (Bradford et al. 2019).

Conclusion and recommendation

Kenya has experienced a roughly 1 °C increase in temperature since the 1970s, while a total of 76,346 km² shifted from a cooler to a warmer zone, a total of 1298 km² shifted from a warmer to a cooler zone, and the hottest zone increased 0.59 °C. Average annual precipitation was relatively stable over the study period, while a total of 136,129 km² shifted from a wetter to a drier zone, a total of 23,317 km² shifted from a drier to a wetter zone, and the average precipitation in the most arid zone decreased 2.57 mm. Overall, more than 36% of all of Kenya's area experienced either shifts in precipitation zones only, shifts in temperature zones only, or shifts in both temperature and precipitation zones. Furthermore, all arid regions expanded from 72% over all of Kenya's area in 1980 to 81% in 2020.

Our analysis can better inform the Kenyan National Climate Change Response Strategy aimed at strengthening nationwide actions towards climate change adaptation, and specifically the National Climate Change Action Plan that is meant to guide the climate actions of the national and county governments and other actors in the country (Kogo et al. 2021). Moreover, the changes we detected have broader global implications in terms of their contribution to global drylands as well as influencing earth system cycles. Overall, examining shifting climate zones is crucial to understanding impacts on agricultural land use and ecosystem change and to devise adaptation strategies and conservation efforts (Bindhu et al. 2021). Furthermore, it can serve as an indication of broader climate change effects on the biosphere, and especially the expansion of drylands globally. Such information can be used to investigate a variety of social and ecological questions that are relevant to agricultural land and ecosystem management, and to reach the UN Sustainable Development Goals.

Supplementary Information The online version contains supplementary material available at <https://doi.org/10.1007/s10113-023-02055-w>.

Acknowledgements This work was supported in part by the Taylor Geospatial Institute and a seed research grant from the Living Earth Collaborative at Washington University in St. Louis. Furthermore, this research was also supported in part by the UK Biotechnology and Biological Sciences Research Council, the Department for International Development, the Economic & Social Research Council, the Medical Research Council, the Natural Environment Research Council, and the Defence Science & Technology Laboratory, under the Zoonoses and Emerging Livestock Systems (ZELS) programme, grant reference BB/L019019/1. This study also received support from the CGIAR One Health initiative "Protecting Human Health Through a One Health Approach," which was supported by contributors to the CGIAR Trust Fund (<https://www.cgiar.org/funders/>). We thank the University of Liverpool's Open Access team for support of the CC-BY open access license for this article.

Data Availability Data used in this study will be made available when possible from the first author.

Declarations

Conflict of interest The authors declare no competing interests.

Open Access This article is licensed under a Creative Commons Attribution 4.0 International License, which permits use, sharing, adaptation, distribution and reproduction in any medium or format, as long as you give appropriate credit to the original author(s) and the source, provide a link to the Creative Commons licence, and indicate if changes were made. The images or other third party material in this article are included in the article's Creative Commons licence, unless indicated otherwise in a credit line to the material. If material is not included in the article's Creative Commons licence and your intended use is not permitted by statutory regulation or exceeds the permitted use, you will need to obtain permission directly from the copyright holder. To view a copy of this licence, visit <http://creativecommons.org/licenses/by/4.0/>.

References

- Abatzoglou JT, Dobrowski SZ, Parks SA, Hegewisch KC (2018) TerraClimate, a high-resolution global dataset of monthly climate and climatic water balance from 1958–2015. *Sci Data* 5:170191. <https://doi.org/10.1038/sdata.2017.191>
- Akter R, Hu W, Gattton M, Bambrick H, Naish S et al (2020) Different responses of dengue to weather variability across climate zones in Queensland, Australia. *Environ Res* 184:109222. <https://doi.org/10.1016/j.envres.2020.109222>
- Ayugi B, Jiang Z, Iyakaremye V, Ngoma H, Babauosmail H et al (2022) East African population exposure to precipitation extremes under 1.5° C and 2.0° C warming levels based on CMIP6 models. *Environmental Research Letters* 17:044051. <https://doi.org/10.1088/1748-9326/ac5d9d>
- Ayugi BO, Wen W, Chepkemoi D (2016) Analysis of spatial and temporal patterns of rainfall variations over Kenya. *J Environ Earth Sci* 6:11. <https://doi.org/10.7176/JEES>
- Beck HE, Zimmermann NE, McVicar TR, Vergopolan N, Berg A et al (2018) Present and future Köppen-Geiger climate classification maps at 1-km resolution. *Sci Data* 5:180214. <https://doi.org/10.1038/sdata.2018.214>
- Bestelmeyer BT, Okin GS, Duniway MC, Archer SR, Sayre NF et al (2015) Desertification, land use, and the transformation of global drylands. *Front Ecol Environ* 13:28–36. <https://doi.org/10.1890/140162>
- Bindhu VM, Smitha PS, Narasimhan B, Annamalai H, Srinivasan G (2021) Koppen-Trewartha climate classification as a diagnostic tool to identify pronounced changes in the projected climate by the General Circulation Model s over India. *Int J Climatol* 41:6616–6639. <https://doi.org/10.1002/joc.7216>
- Bradford JB, Schlaepfer DR, Lauenroth WK, Palmquist KA, Chambers JC et al (2019) Climate-driven shifts in soil temperature and moisture regimes suggest opportunities to enhance assessments of dryland resilience and resistance. *Front Ecol Evol* 7:358. <https://doi.org/10.3389/fevo.2019.00358>
- Bryan E, Ringler C, Okoba B, Roncoli C, Silvestri S et al (2013) Adapting agriculture to climate change in Kenya: household strategies and determinants. *J Environ Manage* 114:26–35. <https://doi.org/10.1016/j.jenvman.2012.10.036>
- Burrell AL, Evans JP, De Kauwe MG (2020) Anthropogenic climate change has driven over 5 million km² of drylands towards desertification. *Nat Commun* 11:3853. <https://doi.org/10.1038/s41467-020-17710-7>
- CCKP (2022) <https://climateknowledgeportal.worldbank.org/country/kenya>. Accessed March 2022
- CDKN (2012) Government of Kenya adaptation technical analysis report. Retrieved April 30, 2019, from <http://www.kccap.info/phocadownload/final/SC3/NCCAP%20Adaptation%20Technical%20Analysis%20Report%20ATAR.pdf>
- Ceglar A, Zampieri M, Toreti A, Dentener F (2019) Observed northward migration of agro-climate zones in Europe will further accelerate under climate change. *Earth's Future* 7:1088–1101. <https://doi.org/10.1029/2019EF001178>
- Chuvieco E (2016) Fundamentals of satellite remote sensing: an environmental approach. CRC Press, Boca Raton
- Cui D, Liang S, Wang D (2021) Observed and projected changes in global climate zones based on Köppen climate classification. *WIREs Clim Change* 12. <https://doi.org/10.1002/wcc.701>
- Dosio A, Mentaschi L, Fischer EM, Wyser K (2018) Extreme heat waves under 1.5 °C and 2 °C global warming. *Environ Res Lett* 13:054006. <https://doi.org/10.1088/1748-9326/aab827>
- Eichsteller M, Njagi T, Nyukuri E (2022) The role of agriculture in poverty escapes in Kenya – developing a capabilities approach in the context of climate change. *World Dev* 149:105705. <https://doi.org/10.1016/j.worlddev.2021.105705>
- ESRI (2022) ArcGIS desktop: release pro, version 2.8.6. Environmental Systems Research Institute, Redlands
- FAO (2019) Trees, forests and land use in drylands: the first global assessment : full report. Food and Agriculture Organization of the United Nations. FAO Forestry Paper No. 184. Rome
- Feng S, Fu Q (2013) Expansion of global drylands under a warming climate. *Atmos Chem Phys* 13:10081–10094. <https://doi.org/10.5194/acp-13-10081-2013>
- Foody GM (2002) Status of land cover classification accuracy assessment. *Remote Sens Environ* 80:185–201. [https://doi.org/10.1016/S0034-4257\(01\)00295-4](https://doi.org/10.1016/S0034-4257(01)00295-4)
- Foody GM (2009) Sample size determination for image classification accuracy assessment and comparison. *Int J Remote Sens* 30:5273–5291. <https://doi.org/10.1080/01431160903130937>
- Fonseca LM, Domingues JP, Dima AM (2020) Mapping the sustainable development goals relationships. *Sustainability* 12:3359. <https://doi.org/10.3390/su12083359>
- Fu C (2017) From climate to global change: following the footprint of Prof. Duzheng YE's research. *Adv Atmos Sci* 34:1159–1168. <https://doi.org/10.1007/s00376-017-6300-6>
- Ghazali D, Guericolas M, Thys F, Sarasin F, Arcos González P et al (2018) Climate change impacts on disaster and emergency medicine focusing on mitigation disruptive effects: an international perspective. *Int J Environ Res Public Health* 15:1379. <https://doi.org/10.3390/ijerph15071379>
- Gikonyo S, Kimani T, Matere J, Kimutai J, Kiambi SG et al (2018) Mapping potential amplification and transmission hotspots for MERS-CoV, Kenya. *EcoHealth* 15:372–387. <https://doi.org/10.1007/s10393-018-1317-6>
- Gorelick N, Hancher M, Dixon M, Ilyushchenko S, Thau D et al (2017) Google Earth Engine: planetary-scale geospatial analysis for everyone. *Remote Sens Environ* 202:18–27. <https://doi.org/10.1016/j.rse.2017.06.031>
- Gosling SN, Arnell NW (2016) A global assessment of the impact of climate change on water scarcity. *Clim Change* 134:371–385. <https://doi.org/10.1007/s10584-013-0853-x>
- Guan Y, Cui W, Liu J, Lu H, Jiang Y et al (2021) Observed changes of Köppen climate zones based on high-resolution data sets in the Qinghai-Tibet Plateau. *Geophys Res Lett* 48. <https://doi.org/10.1029/2021GL096159>
- Guo Y, Abdalla M, Espenberg M, Hastings A, Hallett P et al (2021) A systematic analysis and review of the impacts of afforestation on soil quality indicators as modified by climate zone, forest type and age. *Sci Total Environ* 757:143824. <https://doi.org/10.1016/j.scitotenv.2020.143824>
- Haile GG, Tang Q, Hosseini-Mogharri S, Liu X, Gebremicael TG, et al (2020) Projected impacts of climate change on drought patterns over East Africa. *Earth's Future* 8. <https://doi.org/10.1029/2020EF001502>
- Hamed KH, Rao RA (1998) A modified Mann-Kendall trend test for autocorrelated data. *J Hydrol* 204:182–196. [https://doi.org/10.1016/S0022-1694\(97\)00125-X](https://doi.org/10.1016/S0022-1694(97)00125-X)
- Hao R, Yu D, Liu Y, Liu Y, Qiao J et al (2017) Impacts of changes in climate and landscape pattern on ecosystem services. *Sci Total Environ* 579:718–728. <https://doi.org/10.1016/j.scitotenv.2016.11.036>
- Heffernan C (2018) Climate change and multiple emerging infectious diseases. *Vet J* 234:43–47. <https://doi.org/10.1016/j.tvjl.2017.12.021>
- Huang J, Li Y, Fu C, Chen F, Fu Q et al (2017) Dryland climate change: recent progress and challenges: dryland climate change. *Rev Geophys* 55:719–778. <https://doi.org/10.1002/2016RG000550>
- Huang J, Yu H, Guan X, Wang G, Guo R (2016) Accelerated dryland expansion under climate change. *Nature Clim Change* 6:166–171. <https://doi.org/10.1038/nclimate2837>

- Hunter J, Franklin S, Luxton S, Loidi J (2021) Terrestrial biomes: a conceptual review. *VCS* 2:73–85. <https://doi.org/10.3897/VCS/2021/61463>
- ICPAC (2022) <http://geoportal.icpac.net>. Accessed March 2022
- Jenkins RLM, Warren RF, Price JT (2021) Addressing risks to biodiversity arising from a changing climate: the need for ecosystem restoration in the Tana River Basin, Kenya. *Plos One* 16:e0254879. <https://doi.org/10.1371/journal.pone.0254879>
- Koeva M, Stöcker C, Crommelinck S, Ho S, Chipofya M et al (2020) Innovative remote sensing methodologies for Kenyan land tenure mapping. *Remote Sens* 12:273. <https://doi.org/10.3390/rs12020273>
- Kogo BK, Kumar L, Koech R (2021) Climate change and variability in Kenya: a review of impacts on agriculture and food security. *Environ Dev Sustain* 23:23–43. <https://doi.org/10.1007/s10668-020-00589-1>
- Lawrence TJ, Morreale SJ, Stedman RC, Louis LV (2020) Linking changes in ejido land tenure to changes in landscape patterns over 30 years across Yucatán, México. *Reg Environ Change* 20:136–149. <https://doi.org/10.1007/s10113-020-01722-6>
- Le Page Y, Vasconcelos M, Palminha A, Melo IQ, Pereira JMC (2017) An operational approach to high resolution agro-ecological zoning in West-Africa. *PLoS One* 12:e0183737. <https://doi.org/10.1371/journal.pone.0183737>
- Li M, Wu P, Sexton DMH, Ma Z (2021) Potential shifts in climate zones under a future global warming scenario using soil moisture classification. *Clim Dyn* 56:2071–2092. <https://doi.org/10.1007/s00382-020-05576-w>
- Mahlstein I, Daniel JS, Solomon S (2013) Pace of shifts in climate regions increases with global temperature. *Nature Clim Change* 3:739–743. <https://doi.org/10.1038/nclimate1876>
- Mailloux NA, Henegan CP, Lsoto D, Patterson KP, West PC et al (2021) Climate solutions double as health interventions. *IJERPH* 18:13339. <https://doi.org/10.3390/ijerph182413339>
- Naumann G, Alfieri L, Wyser K, Mentaschi L, Betts RA et al (2018) Global changes in drought conditions under different levels of warming. *Geophys Res Lett* 45:3285–3296. <https://doi.org/10.1002/2017GL076521>
- Nechifor V, Ramos MP, Ferrari E, Laichena J, Kihui E et al (2021) Food security and welfare changes under COVID-19 in sub-Saharan Africa: impacts and responses in Kenya. *Glob Food Sec* 28:100514. <https://doi.org/10.1016/j.gfs.2021.100514>
- Ngoma H, Ayugi B, Onyutha C, Babausmail H, Lim Kam Sian KT et al (2022) Projected changes in rainfall over Uganda based on CMIP6 models. *Theoret Appl Climatol* 149:1117–1134. <https://doi.org/10.1007/s00704-022-04106-4>
- Ngugi RK, Nyariki DM (2005) Rural livelihoods in the arid and semi-arid environments of Kenya: sustainable alternatives and challenges. *Agric Hum Values* 22:65–71. <https://doi.org/10.1007/s10460-004-7231-2>
- Nicholson SE (2018) The ITCZ and the seasonal cycle over equatorial Africa. *Bull Am Meteor Soc* 99:337–348. <https://doi.org/10.1175/bams-d-16-0287.1>
- Olofsson P, Foody GM, Herold M, Stehman SV, Woodcock CE et al (2014) Good practices for estimating area and assessing accuracy of land change. *Remote Sens Environ* 148:42–57. <https://doi.org/10.1016/j.rse.2014.02.015>
- Olofsson P, Foody GM, Stehman SV, Woodcock CE (2013) Making better use of accuracy data in land change studies: estimating accuracy and area and quantifying uncertainty using stratified estimation. *Remote Sens Environ* 129:122–131. <https://doi.org/10.1016/j.rse.2012.10.031>
- Prävalie R (2016) Drylands extent and environmental issues. A global approach. *Earth Sci Rev* 161:259–278. <https://doi.org/10.1016/j.earscirev.2016.08.003>
- Rana VK, Venkata Suryanarayana TM (2020) Performance evaluation of MLE, RF and SVM classification algorithms for watershed scale land use/land cover mapping using sentinel 2 bands. *Remote Sensing Applications: Society and Environment* 19:100351. <https://doi.org/10.1016/j.rsase.2020.100351>
- Richards JA (2013) Remote sensing digital image analysis: an introduction, 5th edn. Springer, Germany
- Seely M, Dirx E, Hager C, Klintonberg P, Roberts C et al (2008) Advances in desertification and climate change research: are they accessible for application to enhance adaptive capacity? *Glob Planet Chang* 64:236–243. <https://doi.org/10.1016/j.gloplacha.2008.07.006>
- Sen PK (1968) Estimates of the regression coefficient based on Kendall's tau. *J Am Stat Assoc* 63:1379–1389. <https://doi.org/10.2307/2285891>
- Shongwe ME, van Oldenborgh GJ, van den Hurk B, van Aalst M (2011) Projected changes in mean and extreme precipitation in Africa under global warming. Part II: East Africa. *J Clim* 24:3718–3733. <https://doi.org/10.1175/2010JCLI2883.1>
- Sisodia PS, Tiwari V, Kumar A (2014) Analysis of supervised maximum likelihood classification for remote sensing image. In *International Conference on Recent Advances and Innovations in Engineering (ICRAIE-2014)*. <https://doi.org/10.1109/icraie.2014.6909319>
- Sombroek WG, Braun HMH, van der Pouw BJA (1982) Exploratory soil map and agro-climatic zone map of Kenya, 1980 (scale 1:1,000,000). Exploratory Soil Survey Report No. E1, Kenya Soil Survey, National Agricultural Laboratories, Ministry of Agriculture, Nairobi
- Spinoni J, Barbosa P, Cherlet M, Forzieri G, McCormick N et al (2021) How will the progressive global increase of arid areas affect population and land-use in the 21st century? *Glob Planet Chang* 205:103597. <https://doi.org/10.1016/j.gloplacha.2021.103597>
- Sylla MB, Elguindi N, Giorgi F, Wisser D (2016) Projected robust shift of climate zones over West Africa in response to anthropogenic climate change for the late 21st century. *Clim Change* 134:241–253. <https://doi.org/10.1007/s10584-015-1522-z>
- Thornton P, Nelson G, Mayberry D, Herrero M (2021) Increases in extreme heat stress in domesticated livestock species during the twenty-first century. *Glob Change Biol* 27:5762–5772. <https://doi.org/10.1111/gcb.15825>
- Thornton P, Nelson G, Mayberry D, Herrero M (2022) Impacts of heat stress on global cattle production during the 21st century: a modelling study. *Lancet Planet Health* 6:e192–e201. [https://doi.org/10.1016/s2542-5196\(22\)00002-x](https://doi.org/10.1016/s2542-5196(22)00002-x)
- Wang C, Li Y, Myint SW, Zhao Q, Wentz EA (2019) Impacts of spatial clustering of urban land cover on land surface temperature across Köppen climate zones in the contiguous United States. *Landsc Urban Plan* 192:103668. <https://doi.org/10.1016/j.landurbplan.2019.103668>
- Wang W, Pijl A, Tarolli P (2022) Future climate-zone shifts are threatening steep-slope agriculture. *Nat Food* 3:193–196. <https://doi.org/10.1038/s43016-021-00454-y>
- Yang D, Yang Y, Xia J (2021) Hydrological cycle and water resources in a changing world: a review. *Geogr Sustain* 2:115–122. <https://doi.org/10.1016/j.geosus.2021.05.003>
- Yao J, Liu H, Huang J, Gao Z, Wang G et al (2020) Accelerated dryland expansion regulates future variability in dryland gross primary production. *Nat Commun* 11:1665. <https://doi.org/10.1038/s41467-020-15515-2>